PENERBIT UMT
Menjana Khazanah Ilmuwan

Journal of Mathematical Sciences and Informatics
Journal Homepage: https://journal.umt.edu.my/index.php/jmsi
eISSN: 2948-3697
DOI: http://doi.org/10.46754/jmsi.2022.12.004

JMSI
Journal of Mathematical Sciences and Informatics

EFFECT OF MARANGONI CONVECTION ON UNSTEADY SQUEEZED FLOW OF WATER BASE CNTs NANOFLUID IN THE PRESENCE OF MAGNETIC FIELD AND VARIABLE THERMAL CONDUCTIVITY OVER A STRETCHING SURFACE

ALI REHMAN[1], ZABIDIN SALLEH[1]* AND USMAN ALI[2]

[1]Special Interest Group for Modelling and Data Analytics, Faculty of Ocean Engineering Technology and Informatics, Universiti Malaysia Terengganu, 21030 Kuala Nerus, Terengganu, Malaysia; alirehmanchd8@gmail.com, zabidin@umt.edu.my. [2]Department of Mathematics, Islami Collage University Peshawar Pakistan; usmanali152221@gmail.com

**Corresponding author: zabidin@umt.edu.my*

ARTICLE INFO

Article History:
Received 9 November 2022
Accepted 8 January 2023
Available online 7 March 2023

Section Editor:
Ilyani Abdullah

Keywords:
Water base CNTs Nanofluid;
OHAM;
Squeezing flow;
MHD;
Stretching surface;
Marangoni convection.

ABSTRACT

This research paper explains the effect of Marangoni convection on the unsteady squeezing flow of water base CNTs for both MWCNT and SWCNT in the presence of a magnetic field and variable thermal conductivity over a stretching surface. The similarity transformation converts the partial differential equation to nonlinear fourth-order ordinary differential equations. The analytical method, namely Optimal Homotopic Analysis Method is used to find the analytical solution of the nonlinear problem that analyses problem. The result of important parameters for both velocity and temperature profiles are plotted and discussed. The BVPh 2.0 package is used to obtain the convergence of the problem up to 25 iterations. The skin friction coefficient and Nusselt number are explained in table form.

2020 Mathematics Subject Classification: 65M25, 76W05

INTRODUCTION

The thermal Marangoni convection is defined as the discrepancy which occurs due to two surface tensions of two fluids, or we can also define it as the discrepancy between two plate surfaces and fluid temperature. The key application of Marangoni convection is silicon melt, precious stone development, atomic reactor spray and coating ignition. Chen [1] used an unstretched sheet to discuss Marangoni convection using the power law model. Rehman *et al.* [2] used a stretching cylinder to discuss Marangoni convection in the unsteady thin film spray of CNT nanofluids by using an analytical method. In the present time, the researcher is interested in squeezing flow because squeezing flow has important applications in fluid mechanics and industry. The applications of squeezing flow are polymer processing, food engineering, physical comparison and injection molding, and biophysical. Kuzma [3] found the effect of fluid inertia by using squeezing flow. Cupta and Gupta [4] investigated squeezing flow using a parallel plate. The researchers [5-8] investigated heat transfer involving squeezing flow. There is some significant use of the study of heat transmission, for example, energy production, heat conduction in tissues, astro physical flow, missiles physical flow and electrical power generation.

Grubka and Bobba [9] investigated heat transfer phenomena using a stretching surface. Dutta [10] discussed hydro magnetic flow and heat transfer by using a stretching sheet. The researchers [11-15] investigated the effect of thermal radiative and heat transfer. Chaim [16] investigated the effect of variable thermal conductivity and heat transfer. Sharma and Singh [17] investigated the effect of MHD flow on a stretching surface. Salahuddin *et al.* [18] discussed the impact of thermal conductivity using a stretching cylinder. Malik *et al.* [19] discussed the effect of MHD Sisko fluid using a stretching cylinder. For energy properties, nanofluids are the active representatives. These fluids play a moving part in developing heat transmission devices operating in several industries and engineering fields. The achievement of energy is not enough but also to adjust the consumption of energy and this is possible only to improve the development of heat transmission liquids, to mechanism the expenditures of energy and to improve the most heat transmission, which is the demand of the industry and other related scientific fields. Former to the application of nanotechnology, analysts and engineers have challenged such huge numbers of questions, recognizing with heat transmission fluids, still, with the development of nanometer size particles, and its uses in the heat transfer fluids have improved thermal conductivity.

Rehman *et al.* [20] used a stretching sheet to discuss the thin film unsteady nanofluid. CNTs are used as a carbon family in this type of research to improve heat transmission. There are two classes of CNTs, the single-wall carbon nanotube (SWCNT) and the multi-wall carbon nanotube (MWCNT). The key use of carbon nanotube (CNT) in engineering for fluidization and heat conversation. Iijima [21] was the first to discover the carbon nanotube (CNT) in 1991. Iijima inspected the first multi-wall carbon nanotube (MWCNT) using the Krastschmer and Huddman method. Later, Donald Bethune 1993 studied multiwall carbon nanotubes (MWCNT) [22]. They discussed the diameter range of single-wall carbon nanotubes and showed that the diameter range of single wall carbon nanotube is $0.4x10^{-9}\ m$ to $3x10^{-9}\ m$ and thickness is about $0.34x10^{-9}\ m$ [23]. In multiwall carbon nanotubes, there are 2 to 50 coaxial nanotubes with a diameter range from $3x10^{-9}\ m$ to $30x10^{-9}\ m$ [24]. Hone [25] investigated that at room temperature, the thermal conductivity of MWCNT is 3000 $Wm^{-1}\ K^{-1}$ and for SWCNT is 6000 $Wm^{-1}\ K^{-1}$. Haq *et al.* [26] discussed the compression of engine base CNT and kerosene oil base CNT, showing that the skin friction of water base CNT is greater than that of the kerosene oil base CNT. Khan *et al.* [27] used a stretching plate to discuss the thermal conductivity and Navier slip boundary condition for CNT.

In this paper, we will explain the effect of Marangoni convection on the unsteady squeezing flow of water base CNTs for both MWCNT and SWCNT in the presence of a magnetic field and variable thermal conductivity over a stretching surface. The Optimal Homotopic Analysis Method (OHAM) is used to find the analytical solution to the nonlinear problem which analyzed problem. The result of important parameters for both velocity and temperature profiles are plotted and discussed. The BVPh 2.0 package is used to obtain the convergences of the problem up to 25 iterations. The skin friction coefficient and Nusselt number are explained in table form.

MATHEMATICAL FORMULATION

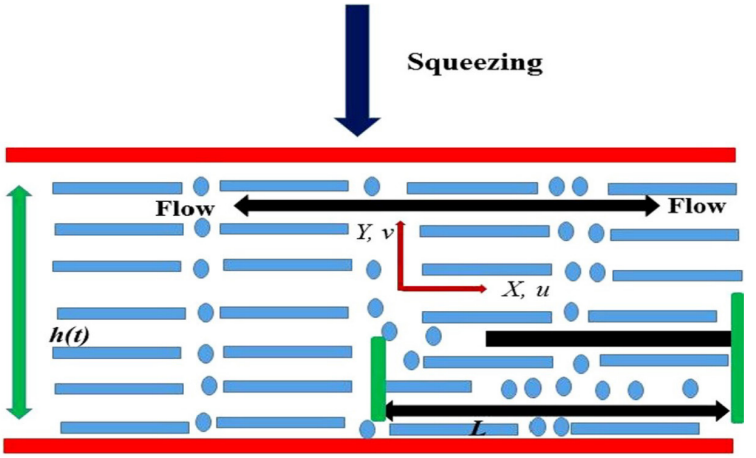

Figure 1: The geometry of the problem

Let us consider the water base CNTs nanofluid of unsteady boundary layer flow. As shown in Figure 1 with a closed squeezed channel with height, $h(t)$, supposed that $h(t)$ is greater than that boundary layer thickness. L represents a micro girder of length which is surrounded classified channel. Further, it is supposed that the squeezing stream is supposed to have occurred from the tip to the surface. Moreover, it is assumed that the lower plate is at rest. The continuity and momentum are settled [28].

$$\frac{\partial u}{\partial x}+\frac{\partial v}{\partial y}=0, \tag{1}$$

$$\frac{\partial u}{\partial t}+u\frac{\partial u}{\partial x}+v\frac{\partial u}{\partial y}=-\frac{1}{p}\frac{\partial p}{\partial x}+\nu(1-n)\frac{\partial^2 u}{\partial y^2}+\sqrt{2}\nu n\Gamma\left(\frac{\partial u}{\partial y}\right)\frac{\partial^2 u}{\partial y^2}-\frac{\sigma B_0^2}{\rho}u, \tag{2}$$

$$\frac{\partial U}{\partial t}+U\frac{\partial U}{\partial x}=-\frac{1}{p}\left(\frac{\partial p}{\partial x}\right)-\frac{\sigma B_0^2}{\rho}U, \tag{3}$$

$$\frac{\partial T}{\partial t}+u\frac{\partial T}{\partial x}+v\frac{\partial T}{\partial y}=\frac{\partial}{\partial y}\left(x(t)\frac{\partial T}{\partial y}\right). \tag{4}$$

Here, u and v are the velocity component in x and y direction, respectively. Kinematic viscosity is denoted by v, the stream velocity is denoted by U, the variable thermal conductivity is denoted by α, the power law index is denoted by n, the time constant is denoted by C, the electric charge density is denoted by ρ, the fluid pressure is denoted by p, and temperature is denoted by T. By eliminating the pressure term from Equation (2) and Equation (3), we obtain:

$$\frac{\partial u}{\partial t}+u\frac{\partial u}{\partial x}+v\frac{\partial u}{\partial y}=\frac{\partial U}{\partial t}+U\frac{\partial U}{\partial x}+\nu(1-n)\frac{\partial^2 u}{\partial y^2}+\sqrt{2}\nu n\Gamma\left(\frac{\partial u}{\partial y}\right)\frac{\partial^2 u}{\partial y^2}+\frac{\sigma B_0^2}{\rho}(U-u), \tag{5}$$

with boundary condition:

$$u(x,0,t) = u_0(t), v(x,0,t) = -v_0(t), -k\frac{\partial T(x,0,t)}{\partial y} = q(x),$$

$$u(x,\infty,t) = U(x,t), T(x,\infty,t) = T_\infty, \tag{6}$$

The free stream temperature, wall heat flux and free stream velocity is denoted by T_∞, $q(x)$ and $U(x,t)$, respectively. $\alpha = \alpha_\infty(1+\varepsilon\theta)$ represents the thermal conductivity. The similarity transformation is defined as:

$$U = ax, \psi = x\sqrt{av}f(\eta), a = \frac{1}{s+bt}, u = axf'(\eta),$$

$$v = -f(\eta)\sqrt{av}, \theta(\eta) = \frac{T-T_\infty}{q_0 x\sqrt{\frac{\nu}{a}}}, \eta = y\sqrt{\frac{a}{\nu}}, \tag{7}$$

where b is the squeezed flow index, s is the arbitrary constant, a shows the strength squeezing flow parameter, heat flux is represented by q_0 and k is the thermal conductivity. Using the similarity transformation (7) into Equation (4) and Equation (5), the partial differential equation is transformed into an ordinarily differential equation.

$$f'''' + (1-\phi)^{2.5}\left(1-\phi+\phi\frac{(\rho_s)_{CNT}}{(\rho_f)_{CNT}}\right)\left(f+\frac{b\eta}{2}\right)f''' - (f')^2 + b(f'-1) + nw_e f''^2(\eta)f'''(\eta) - M(1-\phi)^{2.5}(1-f') = 0, \tag{8}$$

$$\frac{k_{nf}}{k_f}\theta'' + Pr\left[(1-\phi)+\phi\frac{(\rho C_p)_{CNT}}{(\rho C_p)_{CNT}}\right]\left(f+\frac{b\eta}{2}\right)\theta' + Pr\varepsilon(\theta')^2 - Pr\left(f'+\frac{b}{2}\right)\theta = 0, \tag{9}$$

with

$$f(0) = -f_0, f'(0) = 0, \theta'(0) = -1,$$

$$f'(\infty) \to 1, \theta(\infty) \to 0, \tag{10}$$

where $Pr = \frac{\nu}{\sigma}$ is Prandtl number, $f_0 = \sqrt{\nu}$ is permeable velocity, $w_e = \frac{\sqrt{2a}\Gamma U}{\sqrt{\nu}}$, $M = \frac{\sigma B_0^2}{\sigma a}$ is a magnetic parameter and n is the power law index.

The coefficient of skin friction and Nusselt number is defined as:

$$\sqrt{Re_x}C_f = \left[(1-n)f''(\eta) + \frac{n}{2}w_e\left(f''(\eta)\right)^2\right]_{\eta=0}, \text{ and } Nu_x\sqrt{Re_x} = -\theta'(\eta)_{\eta=0}, \tag{11}$$

METHOD OF SOLUTION

The given Equations (8) and (9) are solved analytically by the analytical method optimal homotopy asymptotic method (OHAM) which is given below:

$$L\big(u(x)\big) + N\big(u(x)\big) + g(x) = 0, B\big(u(x)\big), \tag{12}$$

where L is the linear operator and x is an independent variable, $g(x)$ is the unknown function, N is the nonlinear operator and $B(u)$ is a boundary operator. By using this method, we first find a family of the equation:

$$H(\phi(x), p) = (1-p)\big[L\big(\phi(x,p)\big) + g(x)\big] - H(p)\big[L\big(\phi(x,p)\big) + g(x) + N\big(\phi(x,p)\big)\big] = 0,$$

$$B\big(\phi(x,p)\big) = 0, \tag{13}$$

where p is an embedding parameter and lies in [0,1], $H(p)$ is a nonzero auxiliary function for $p \neq 0$, $H(0) = 0$ and $\emptyset(x,p)$ is an unknown function. Using the initial guessed values and auxiliary linear operators from Equations (8) and (9),

$$f_0(\eta) = \frac{(b-m)}{24}\eta^4 + \frac{c_2\eta^2}{2} - f_0 = 0, \tag{14}$$

$$L_f = \frac{d^4 f}{d\eta^4}, L_\theta = \frac{d^2\theta}{d\eta^2}, \tag{15}$$

with constant properties

$$L_f(C_1 + C_2\eta + C_3\eta^2 + C_4\eta^3) = 0 \text{ ,and } L_\theta(C_5 + C_6\eta) = 0, \tag{16}$$

where C_i (i = 1,2,...,6) are arbitrary constant which is included in the general solution.

The average squared residuals error is presented by Liao [29], so, the Equations (8) and (9) can be written as:

$$\varepsilon_m^f = \frac{1}{n+1}\sum_{j=1}^{n}\left[\kappa_f\left(\sum_{j=1}^{n} f(\eta)_{\eta=j\delta\eta}\right)\right], \tag{17}$$

$$\varepsilon_m^\theta = \frac{1}{n+1}\sum_{j=1}^{n}\left[\kappa_\theta\left(\sum_{j=1}^{n} f(\eta)_{\eta=j\delta\eta}, \sum_{j=1}^{n}\theta(\eta)_{\eta=j\delta\eta}\right)\right], \tag{18}$$

$$\varepsilon_m^t = \varepsilon_m^f + \varepsilon_m^\theta. \tag{19}$$

RESULTS AND DISCUSSION

Table 1: Comparison of the skin friction for the two nanofluids when $Pr = 5.6$, $w_e = 0.1$, $\varepsilon = 1$

b	*M*	*MWCNT*	*SWCNT*
0.7	0.5	0.339705	0.29471
0.8		0.32164	0.279547
0.9		0.31147	0.27264
	0.6	0.3100877	0.26994
	0.7	0.30608	0.23724
		0.298432	0.2246
		0.25818	0.21641

Table 2: Comparison of the Nusselt number ($Re_x^{-1/2} Nu_x$) for the two nanofluids when $f_0 = 0.1$, $M = 0.2$, $b = 0.5$

Pr	w_e	*MWCNT*	*SWCNT*
5	0.3	0.41231	0.39077
7		0.39341	0.38237
9		0.37451	0.37397
	0.5	0.35614	0.35647
	0.7	0.33776	0.34897
		0.32795	0.33121
		0.31021	0.31346

Table 3: Show convergence of the method for SWCNT when $Pr = 7$, $M = 1$, $f_0 = 0.5$, $\emptyset = 0.1$, $\varepsilon = 0.01$

m	ε^f_m *SWCNT*	ε^θ_m *SWCNT*
5	7.55438×10^{-1}	3.86775×10^{-1}
10	4.69094×10^{-3}	6.48738×10^{-2}
15	3.209443×10^{-7}	5.07298×10^{-4}
20	5.37298×10^{-9}	1.54131×10^{-5}
25	9.33787×10^{-11}	9.94423×10^{-6}

Table 4: Show the convergence of the method for MWCNT when $Pr = 9$, $M = 3$, $w_e = 0.9$ $\emptyset = 0.1$, $\varepsilon = 0.05$

m	ε^f_m *MWCNT*	ε^θ_m *MWCNT*
5	1.18991×10^{-1}	7.88574×10^{-1}
10	5.47666×10^{-2}	5.0759×10^{-3}
15	4.53983×10^{-3}	3.0759×10^{-5}
20	7.4616×10^{-4}	6.55721×10^{-7}
25	7.19521×10^{-5}	8.226632×10^{-9}

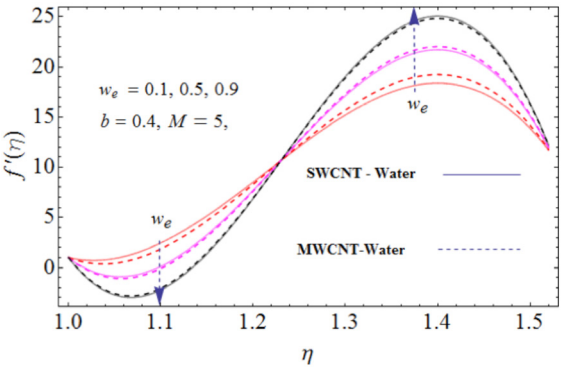

Figure 2: Effect of Weissenberg number on the velocity profile

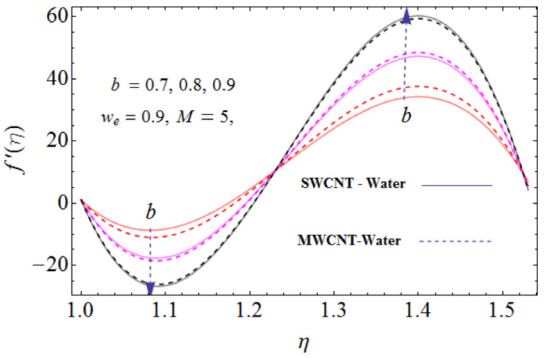

Figure 3: Effect of squeezed flow index on the velocity profile

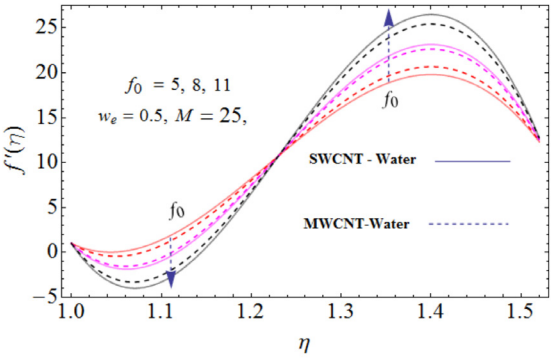

Figure 4: Effect of permeable velocity on the velocity profile

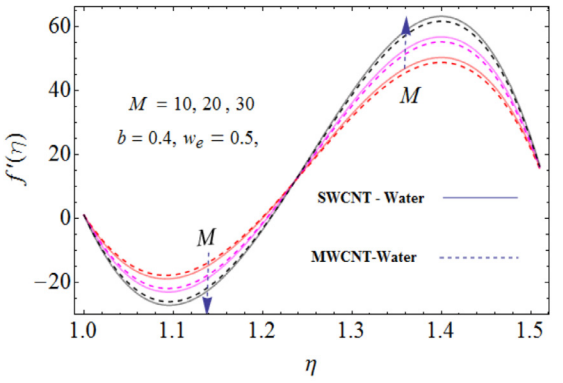

Figure 5: Effect of magnetic parameter on the velocity profile

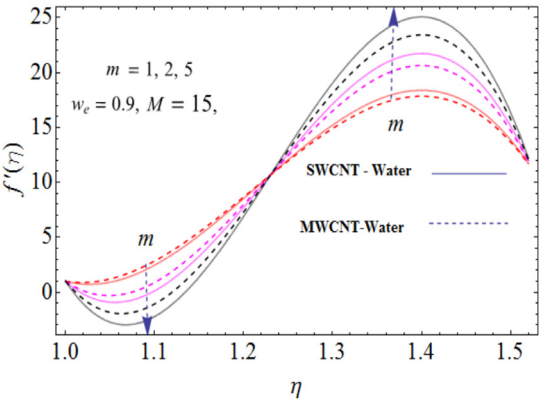

Figure 6: Effect of Marangoni convection parameter on the velocity profile

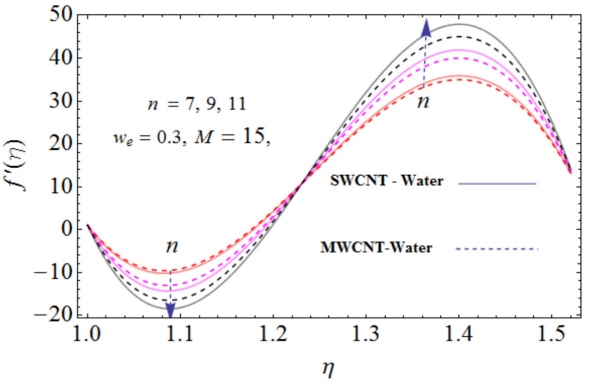

Figure 7: Effect of power law index on the velocity profile

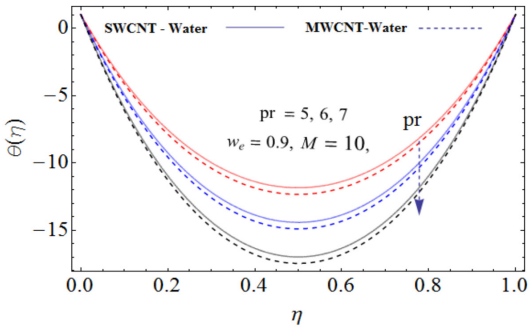

Figure 8: Effect of Prandtl number on the temperature profile

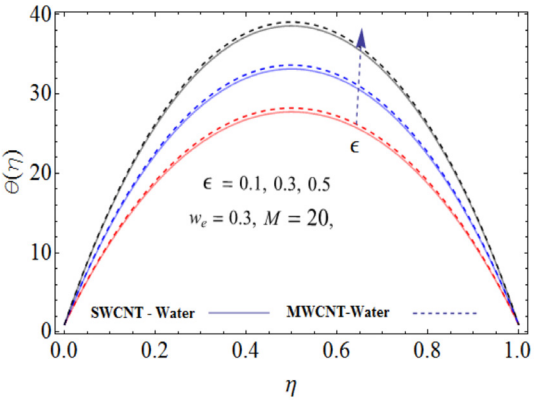

Figure 9: Effect of ε on the temperature profile

The central objective of this section is to study the result of several model issues like M, f_0, Pr, w_e, ε, n, b, m (magnetic parameter, permeable velocity, Prandtl number, Weissenberg number, small quantity, power law index, squeezed flow index and Marangoni convection parameter on velocity and temperature distribution). In Tables 1 and 2, the numeric results illustrate the impacts of different model factors on the skin friction coefficient and Nusselt number of both MWCNT and SWCNT. The effect of different parameters on the local skin friction coefficient is shown in Table 1. Table 1 depicts the skin friction coefficient decreasing in b whereas Table 2 shows the Nusselt number coefficient decreasing in both MWCNT and SWCNT for the increasing value of the Prandtl number and Weissenberg number. The convergence for MWCNT and SWCNT nanofluid up to the 25th iteration has been obtained for the SWCNT and MWCNT nanofluid in Tables 3 and 4, one by one. Tables 3 and 4 show that increasing the number of iterations reduces the order of residual error and the strong convergence attained.

Figure 2 shows the influence of the Weissenberg number on the velocity profile. Increasing the Weissenberg number decreases the velocity profile. This effect is partial; after the critical point, the velocity field increases, as shown in Figure 2. Figure 3 shows the effect of squeezed flow index on the velocity profile. Increasing the squeezed flow index decreases the velocity profile primarily due to Marangoni convection. This consequence is also partial; after the critical point, the velocity field increases, as seen in Figure 3. Figure 4 shows the effect of permeable velocity on the velocity

profile. Increasing permeable velocity decreases the velocity profile primarily due to Marangoni convection. This effect is partial; after the critical point, the velocity field increases, which plays an important role in heat transfer. Figure 5 shows the impact of the magnetic parameter on the velocity profile. Increasing magnetic parameter decreases the velocity profile primarily due to Marangoni convection. This consequence is partial and the velocity field increases after the critical point, which plays an important role in heat transfer.

Figure 6 shows the consequence of the Marangoni convection parameter on the velocity profile. Increasing the Marangoni convection parameter decreases the velocity profile primarily due to Marangoni convection. This effect is partial; after the critical point, the velocity field increases, which plays an important role in heat transfer. Figure 7 shows the consequence of the power law index n on the velocity profile. By increasing the power law index parameter n, the velocity profile decreases primarily due to Marangoni convection. This effect is partial; after the critical point, the velocity field increases, which plays an important role in heat transfer. Figure 8 shows the effect of the Pr against the $\theta(\eta)$ temperature field. The relation between the temperature field and Pr is inversely related. So, by enhancing the Pr, decreasing the temperature profile as displayed in Figure 8. Figure 9 shows the effect of ε on the temperature profile. The relation between ε and temperature is directly related. By increasing ε, the temperature profile increases because by increasing the small partial, the kinetic energy of the fluid particle increases the variation of thermal characteristics. So, as a result, the temperature profile increase.

CONCLUSION

This paper explains the effect of Marangoni convection on the unsteady squeezing flow of water-based nanofluid CNTs for both MWCNT and SWCNT in the presence of a magnetic field and variable thermal conductivity. The partial differential equation is converted using the similarity transformation to a nonlinear fourth-order ordinary differential equation. The analytical method (OHAM) is used to find the analytical solution to the nonlinear problem, which analyzes the problem. The result of important parameters for both velocity and temperature profiles are plotted and discussed. The BVPh 2.0 package is used to obtain the convergence of the problem up to 25 iterations. The skin friction coefficient and Nusselt number are explained in table form. The obtained outputs are deliberated as follows:

- It is observed that the increasing Weissenberg number decreases the velocity field but due to Marangoni convection, this effect is changed and after some point, the velocity field increases.
- It is observed that increasing the squeezed flow index decreases the velocity profile but due to Marangoni convection, this effect changes and the velocity field increases after some point.
- It is observed that increasing the magnetic field's values decreases the velocity profile but due to Marangoni convection, this effect changes and the velocity field increases.
- It is observed that increasing the Prandtl number, Pr, decreases the temperature profile.
- By increasing the ε, increases the temperature field.

CONFLICTS OF INTEREST

The authors declare no conflict of interest. The funders had no role in the design of the study; in the collection, analyses, or interpretation of data; in the writing of the manuscript, or in the decision to publish the results.

ACKNOWLEDGEMENTS

The authors appreciate the support of their institutions. They gratefully acknowledge the Ministry of Higher Education Malaysia and Universiti Malaysia Terengganu for their financial support.

REFERENCES

[1] Chen, C. H. (2007). Marangoni effects on forced convection of power-law liquids in a thin film over a stretching surface. *Physics Letters A, 370*(1), 51-57. https://doi.org/10.1016/j.physleta.2007.05.024

[2] Rehman, A., Gul, T., Salleh, Z., Mukhtar, S., Hussain, F., Nisar, K. S., & Kumam, P. (2019). Effect of the Marangoni convection in the unsteady thin film spray of CNT nanofluids. *Processes, 7*(6), 392. http://dx.doi.org/10.3390/pr7060392

[3] Kuzma, D. C. (1968). Fluid inertia effects in squeeze films. *Applied Scientific Research, 18*, 15–20. https://doi.org/10.1007/BF00382330

[4] Gupta, P. S., & Gupta, A. S. (1977). Squeezing flow between parallel plates. *Wear, 45,* 177–185.

[5] Wang, C. Y., & Watson, L. T. (1979). Squeezing of a viscous fluid between elliptic plates. *Applied Scientific Research, 35,* 195–207. https://doi.org/10.1007/BF00382705

[6] Bhattacharyya, S. & Pal, A. (1997). Unsteady MHD squeezing flow between two parallel rotating discs. *Mechanics Research Communications, 24*(6), 615–623.

[7] Xu, C., Yuan, L., Xu. Y., & W. Hang. ((2010). Squeeze flow of interstitial Herschel-Bulkley fluid between two rigid spheres. *Particuology, 8*(4), 360–364. https://doi.org/10.1016/j.partic.2009.07.008

[8] Ganji, D. D., Abbasi, M., Rahimi, J., Gholami, M., & Rahimipetroudi, I. (2014). On the MHD squeeze flow between two parallel disks with suction or injection via HAM and HPM. *Frontiers of Mechanical Engineering, 9*(3) (2014), 270–280.

[9] Grubka, L. J., & Bobba, K. M. (1985). Heat transfer characteristics of a continuous, stretching surface with variable temperature. *Journal Heat Transfer, 107,* 248–250.

[10] Dutta, B. K. (1988). Heat transfer from a stretching sheet in hydromagnetic flow. *Wärme-und Stoffübertragung, 23*(1), 35-37. https://doi.org/10.1007/BF01460746

[11] Rudraswamy, N. G., Ganesh Kumar, K., Gireesha, B. J., & Gorla, R. S. R. (2017). Combined effect of joule heating and viscous dissipation on MHD three dimensional flow of a Jeffrey nanofluid. *Journal of Nanofluids, 6*(2), 300–310.

[12] Rudraswamy, N. G., & Gireesha, B. J. (2014). Influence of chemical reaction and thermal radiation on MHD boundary layer flow and heat transfer of a nanofluid over an exponentially stretching sheet. *Journal of Applied Mathematics and Physics, 2*(2), 24-32.

[13] Kuiry, D. R., & Bahadur, S. (2015). Steady MHD flow of viscous fluid between two parallel porous plates with heat transfer in an inclined magnetic field. *Journal of Scientific Research, 7*(3), 21–31. https://doi.org/10.3329/jsr.v7i3.22574

[14] Rudraswamy, N. G., Ganesh Kumar, K., Gireesha, B. J., & Gorla, R. S. R. (2016). Soret and Dufour effects in three-dimensional flow of Jeffery nanofluid in the presence of nonlinear thermal radiation. *Journal of Nanoengineering and Nanomanufacturing, 6*(4), 278–287.

[15] Kumar, K. G., Rudraswamy, N. G., Gireesha, B. J., & Krishnamurthy, M. R. (2017). Influence of nonlinear thermal radiation and viscous dissipation on three-dimensional flow of Jeffrey nanfluid over a stretching sheet in the presence of Joule heating. *Nonlinear Engineering, 6*(3). http://dx.doi.org/10.1515/nleng-2017-0014

[16] Chaim, T. C. (1998). Heat transfer in a fluid with variable thermal conductivity over stretching sheet. *Acta Mechanica, 129*(1-2), 63–72.

[17] Sharma, P. R., & Singh, G. (2009). Effects of variable thermal conductivity and heat source/sink on MHD flow near a stagnation point on a linearly stretching sheet. *Journal of Applied Fluid Mechanics, 2*(1), 13–21.

[18] Salahuddin, T., Malik, M. Y., Hussain A., Bilal, S, & Awais, M. (2016). Combined effects of variable thermal conductivity and MHD flow on pseudoplastic fluid over a stretching cylinder by using Keller box method. *Information Sciences Letters, 5*(1), 11-19.

[19] Malik, M. Y., Hussain, A., Salahuddin, T., Awais, M., & Bilal, S. (2016). Magnetohydrodynamic flow of Sisko fluid over a stretching cylinder with variable thermal conductivity: A numerical study. *AIP Advances, 6,* 025316. https://doi.org/10.1063/1.4942476

[20] Rehman, A., Salleh, Z., Gul, T., & Zaheer, Z. (2019). The Impact of Viscous Dissipation on the thin film unsteady flow of GO-EG/GO-W Nanofluids. *Mathematics, 7,* 653. https://doi.org/10.3390/math7070653

[21] Iijima, S. (1991). Helical microtubules of graphitic carbon. *Nature, 354,* 56-58. https://doi.org/10.1038/354056a0

[22] Ajayan, P., lijima, S. (1993). Capillarity-induced filling of carbon nanotubes. *Nature, 361,* 333-334. https://doi.org/10.1038/361333a0

[23] To, C. W. S. (2006). Bending and shear moduli of single–walled carbon nanotubes. *Finite Elements in Analysis and Design, 42*(5), 404–413. https://doi.org/10.1016/j.finel.2005.08.004

[24] Dresselhaus, M. S., Dresselhaus, G., & Saito, R. (1995). Physics of carbon nanotubes. *Carbon, 33*(7), 883–891.

[25] Hone, J. (2004). Carbon nanotubes: Thermal properties. *Dekker Encyclopedia of Nanoscience and Nanotechnology, 7,* 603–610.

[26] Haq. R. U., Nadeem, S., Khan, Z. H., & Noor, N. F. M. (2015). Convective heat transfer in MHD slip flow over a stretching surface in the presence of carbon nanotubes. *Physica B Condensed Matter, 457,* 40–47. https://doi.org/10.1016/j.physb.2014.09.031

[27] Khan, W. A., Khan, Z. H., & Rahi, M. (2014). Fluid flow and heat transfer of carbon nanotubes along a flat plate with Navier slip boundary. *Applied Nanoscience, 4,* 633–641. https://doi.org/10.1007/s13204-013-0242-9

[28] Kumar, K. G., Gireesha, B. J., Krishanamurthy, M. R., & Rudraswamy, N. G. (2017). An unsteady squeezed flow of a tangent hyperbolic fluid over a sensor surface in the presence of variable thermal conductivity. *Results in Physics, 7,* 3031-3036. https://doi.org/10.1016/j.rinp.2017.08.021

[29] Liao, S. J. (2010). An optimal homotopy-analysis approach for strongly nonlinear differential equations. *Communications in Nonlinear Science and Numerical Simulation, 15,* 2003–2016.